SUPPLEMENTARY MATERIAL

S1. Poisson-process ('P_Sequence') deposition model coding applied to our new TP-2005 ^{14}C data

```
 Options()
 {
  Curve="Hulu Cave.14c";                    (Cheng et al., 2018)   (model A)
  Curve="IntCal13.14c";                     (Reimer et al., 2013)  (model B)
  kIterations=1000;
 };
 Plot()
 {
  Outlier_Model("RScaled", T(5), U(0,4), "r");
  Outlier_Model("SSimple", N(0,2), 0, "s");
  P_Sequence("TP-2005 (Staff et al., 2019)", 100, 10, U(-2,2))
  {
   Boundary("14.80m")
   {
    z=14.800;
   };
   R_F14C("OxA-29699", 0.00348, 0.00056)
   {
    Outlier("RScaled", 0.05);
    z=14.775;
   };
```

etc…

```
   R_Combine("OxA-29319/OxA-29320")
   {
    R_F14C("OxA-29319", 0.01384, 0.00059)
    {
     Outlier("SSimple", 0.05);
    };
    R_F14C("OxA-29320", 0.01472, 0.00062)
    {
     Outlier("SSimple", 0.05);
    };
    Outlier("RScaled", 0.05);
    z=12.925;
   };
   R_F14C("OxA-29318", 0.01383, 0.00057)
   {
    Outlier("RScaled", 0.05);
    z=12.909;
   };
   R_F14C("OxA-28873", 0.01384, 0.00071)
   {
    Outlier("RScaled", 0.05);
    z=12.886;
   };
   Boundary("12.87m (Campanian Ignimbrite)")
   {
    z=12.870;
   };
  };
 };
```

S2. Poisson-process ('P_Sequence') deposition model coding applied to the previously published TP-2005 ^{14}C data of Müller et al. (2011)

```
 Options()
 {
  Curve="Hulu Cave.14c";                    (Cheng et al., 2018)   (model C)
  Curve="IntCal13.14c";                     (Reimer et al., 2013)  (model D)
  kIterations=1000;
 };
 Plot()
 {
  Outlier_Model("RScaled", T(5), U(0,4), "r");
  Outlier_Model("SSimple", N(0,2), 0, "s");
  P_Sequence("TP-2005 (Müller et al., 2011) lower", 100, 10, U(-2,2))
  {
   Boundary("15.30m")
   {
    z=15.30;
   };
   R_Date("Beta-246628", 43100, 1200)
   {
    Outlier("RScaled", 0.05);
    z=15.28;
   };
```

etc…

```
   R_Date("Beta-244643", 35290, 350)
   {
    Outlier("RScaled", 0.05);
    z=13.30;
   };
   Boundary("12.87m (Campanian Ignimbrite)")
   {
    z=12.87;
   };
  };
  P_Sequence("TP-2005 (Müller et al., 2011) upper",100,10,U(-2,2))
  {
   Boundary("=12.87m (Campanian Ignimbrite)")
   {
    z=12.64;
   };
   R_Date("Beta-244642", 32390, 260)
   {
    Outlier("RScaled", 0.05);
    z=11.85;
   };
```

etc…

```
   Boundary("0.50m")
   {
    z=0.50;
   };
  };
 };
```

S3. Supporting uniform ('U_Sequence') deposition model coding applied to our new TP-2005 ^{14}C data

```
 Options()
 {
  Curve="Hulu Cave.14c";                          (Cheng et al., 2018)   (model E)
  Curve="IntCal13.14c";                           (Reimer et al., 2013)  (model F)
  kIterations=1000;
 };
 Plot()
 {
  Outlier_Model("RScaled", T(5), U(0,4), "r");
  Outlier_Model("SSimple", N(0,2), 0, "s");
  U_Sequence("TP-2005 (Staff et al., 2019)")
  {
   Boundary("14.80m")
   {
    z=14.800;
   };
   R_F14C("OxA-29699", 0.00348, 0.00056)
   {
    Outlier("RScaled", 0.05);
    z=14.775;
   };

etc…

   R_Combine("OxA-29319/OxA-29320")
   {
    R_F14C("OxA-29319", 0.01384, 0.00059)
    {
     Outlier("SSimple", 0.05);
    };
    R_F14C("OxA-29320", 0.01472, 0.00062)
    {
     Outlier("SSimple", 0.05);
    };
    Outlier("RScaled", 0.05);
    z=12.925;
   };
   R_F14C("OxA-29318", 0.01383, 0.00057)
   {
    Outlier("RScaled", 0.05);
    z=12.909;
   };
   R_F14C("OxA-28873", 0.01384, 0.00071)
   {
    Outlier("RScaled", 0.05);
    z=12.886;
   };
   Boundary("12.87m (Campanian Ignimbrite)")
   {
    z=12.870;
   };
  };
 };
```

Table S1. Previous AMS ^{14}C dates from Tenaghi Philippon core TP-2005, as published by Müller et al. (2011)

Depth (m)	Material	AMS Laboratory Code	Conventional ^{14}C Age (yrs BP ± 1σ) (Stuiver and Polach, 1977)
0.76	*Viviparus contectus*	Poz-15890	1,950 ± 30
1.79	*Oxyloma elegans*	Poz-15891	4,200 ± 40
3.41	*Oxyloma elegans*	Poz-15894	5,790 ± 40
4.20	wood	Beta-244646	6,350 ± 50
4.59	wood	Beta-244647	7,600 ± 50
5.56	wood	Beta-244650	8,820 ± 50
6.15	wood	Beta-244651	9,890 ± 60
6.98	bulk peat	Beta-244654	13,570 ± 70
7.18	bulk peat	Beta-244655	16,560 ± 90
8.20	bulk peat	Beta-244637	20,220 ± 100
8.86	bulk peat	Poz-16295	23,330 ± 150
9.30	bulk peat	Beta-244638	24,310 ± 160
9.85	bulk peat	Beta-244639	25,120 ± 150
10.60	bulk peat	Beta-244640	27,760 ± 190
11.25	bulk peat	Beta-244641	28,680 ± 230
11.85	bulk peat	Beta-244642	32,390 ± 260
13.30	bulk peat	Beta-244643	35,290 ± 350
13.83	bulk peat	Beta-244644	36,520 ± 400
14.65	bulk peat	Beta-244645	39,570 ± 570
15.28	bulk peat	Beta-246628	43,100 ± 1,200

Table S2. New AMS ^{14}C dates of homogenised peat samples from Tenaghi Philippon core TP-2005. Samples marked with an asterisk (*) are supporting measurements of the base-soluble humic acid component extracted from the peat (see section 3.2 of the main text). The sample marked with a dagger (†) produced a low target current in the AMS, and so should be treated with caution (and hence the 'OxA-X-' laboratory code prefix).

Depth (m)	AMS Laboratory Code	Conventional ^{14}C Age (yrs BP ± 1σ) (Stuiver and Polach, 1977)	$F^{14}C$ (± 1σ) (Reimer et al., 2004)	$\delta^{13}C$ (‰)
12.87-12.90	OxA-28872 *	34,290 ± 370	0.01400 ± 0.00064	-27.7
12.87-12.90	OxA-28873	34,400 ± 400	0.01384 ± 0.00071	-26.4
12.90-12.92	OxA-29318	34,390 ± 330	0.01383 ± 0.00057	-27.4
12.92-12.94	OxA-29319	34,380 ± 340	0.01384 ± 0.00059	-26.6
12.92-12.94	OxA-29320	33,890 ± 340	0.01472 ± 0.00062	-26.7
12.94-12.97	OxA-29321	34,490 ± 340	0.01365 ± 0.00058	-26.8
12.97-13.00	OxA-29322	34,880 ± 370	0.01300 ± 0.00061	-26.8
13.00-13.05	OxA-29323	35,050 ± 360	0.01274 ± 0.00057	-26.8
13.05-13.10	OxA-29324	36,650 ± 450	0.01045 ± 0.00058	-27.1
13.10-13.15	OxA-29325	36,350 ± 450	0.01080 ± 0.00061	-27.1
13.15-13.20	OxA-29326	36,650 ± 450	0.01047 ± 0.00059	-27.2
13.20-13.25	OxA-29327	35,900 ± 450	0.01149 ± 0.00063	-27.2
13.25-13.30	OxA-28874 *	35,640 ± 330	0.01184 ± 0.00049	-27.2
13.25-13.30	OxA-28847	37,600 ± 900	0.00929 ± 0.00104	-27.3
13.25-13.30	OxA-29603	36,100 ± 400	0.01114 ± 0.00057	-26.9
13.30-13.35	OxA-29328	36,300 ± 450	0.01092 ± 0.00059	-27.0
13.35-13.40	OxA-29329	36,250 ± 450	0.01096 ± 0.00065	-26.8
13.40-13.45	OxA-29330	37,250 ± 500	0.00969 ± 0.00058	-26.8
13.45-13.50	OxA-29331	36,650 ± 450	0.01045 ± 0.00062	-26.6
13.50-13.55	OxA-29364	37,350 ± 500	0.00954 ± 0.00060	-27.0
13.55-13.60	OxA-29365	38,400 ± 550	0.00840 ± 0.00057	-26.7
13.60-13.65	OxA-29366	38,850 ± 550	0.00796 ± 0.00053	-26.6
13.65-13.70	OxA-29367	39,000 ± 650	0.00780 ± 0.00063	-26.4
13.70-13.75	OxA-29368	39,900 ± 600	0.00694 ± 0.00052	-26.5
13.75-13.80	OxA-28875 *	40,200 ± 500	0.00670 ± 0.00040	-27.3
13.75-13.80	OxA-28876	40,800 ± 900	0.00626 ± 0.00068	-27.1
13.80-13.85	OxA-29369	39,950 ± 650	0.00693 ± 0.00054	-27.0
13.85-13.90	OxA-29679	40,700 ± 1300	0.00629 ± 0.00101	-27.7
13.85-13.90	OxA-29604	39,400 ± 600	0.00741 ± 0.00053	-27.1
13.90-13.95	OxA-29370	40,600 ± 650	0.00638 ± 0.00051	-26.9
13.95-14.00	OxA-29371	40,900 ± 800	0.00614 ± 0.00062	-27.2
14.00-14.05	OxA-29372	42,100 ± 900	0.00531 ± 0.00060	-27.0
14.05-14.10	OxA-29373	42,800 ± 1,000	0.00485 ± 0.00061	-27.2
14.10-14.15	OxA-29374	43,200 ± 800	0.00460 ± 0.00046	-26.9
14.15-14.20	OxA-30603	43,500 ± 900	0.00442 ± 0.00052	-27.0
14.20-14.25	OxA-30604	41,700 ± 900	0.00554 ± 0.00062	-27.2
14.25-14.30	OxA-30605	41,200 ± 900	0.00589 ± 0.00068	-26.9
14.30-14.35	OxA-30606	42,600 ± 900	0.00495 ± 0.00057	-27.2
14.35-14.40	OxA-30607	41,200 ± 900	0.00590 ± 0.00065	-27.0

Depth (m)	AMS Laboratory Code	Conventional ^{14}C Age (yrs BP ± 1σ) (Stuiver and Polach, 1977)	$F^{14}C$ (± 1σ) (Reimer et al., 2004)	$\delta^{13}C$ (‰)
14.40-14.45	OxA-30761	42,200 ± 1,200	0.00526 ± 0.00078	-27.7
14.45-14.50	OxA-30762	42,900 ± 1,100	0.00481 ± 0.00068	-27.5
14.50-14.55	OxA-30763	42,900 ± 1,000	0.00481 ± 0.00060	-27.3
14.55-14.60	OxA-30764	44,300 ± 1,200	0.00405 ± 0.00059	-27.5
14.60-14.65	OxA-30765	43,700 ± 1,100	0.00431 ± 0.00061	-27.3
14.65-14.70	OxA-29698	44,500 ± 1,100	0.00393 ± 0.00053	-27.6
14.70-14.75	OxA-30766	45,600 ± 1,200	0.00344 ± 0.00053	-27.3
14.75-14.80	OxA-29699	45,500 ± 1,300	0.00348 ± 0.00056	-27.8
19.50-19.55	OxA-28848 *	>46,900	0.00107 ± 0.00093	-28.3
19.50-19.55	OxA-28877	>55,900	0.00000 ± 0.00048	-27.6
19.50-19.55	OxA-29332	>52,800	0.00028 ± 0.00056	-27.4
19.50-19.55	OxA-30767	>52,100	0.00053 ± 0.00049	-27.4
19.50-19.55	OxA-29396	>56,400	0.00000 ± 0.00045	-27.4
19.50-19.55	OxA-X-2558-22 *†	47,600 ± 3,100	0.00268 ± 0.00103	-27.8
19.50-19.55	OxA-30608	>53,800	0.00025 ± 0.00049	-27.6

182

Table S3. Hulu Cave (Cheng et al., 2018) modelled ages for our contiguous, homogenised peat samples from Tenaghi Philippon core TP-2005, as derived from the primary `P_Sequence` (model A) and supporting `U_Sequence` (model E) deposition models in OxCal ver. 4.3 (Bronk Ramsey, 2008, 2019; Bronk Ramsey and Lee, 2013). (N.b. the supporting measurements of the base-soluble humic acid component extracted from the peat, as given in Table S2, were not included in the Bayesian modelling.) For simplicity, the modelled data are presented at the 68.2% highest probability density ranges. Posterior `Outlier` probabilities for each ^{14}C determination are given, as compared to the prior 5% probabilities applied to each sample.

Depth (m)	AMS Laboratory Code	Hulu Cave modelled age (cal. BP) using primary `P_Sequence` deposition model (68.2% range)	Posterior/prior `Outlier` probability (%)	Hulu Cave modelled age (cal. BP), using supporting `U_Sequence` deposition model (68.2% range)	Posterior/prior `Outlier` probability (%)
12.87-12.90	OxA-28873	39,034 – 38,617	4 / 5	39,741 – 39,448	4 / 5
12.90-12.92	OxA-29318	39,125 – 38,715	4 / 5	39,830 – 39,544	4 / 5
12.92-12.94	OxA-29319	39,210 – 38,792	3 / 5	39,894 – 39,612	3 / 5
	OxA-29320		10 / 5		5 / 5
12.94-12.97	OxA-29321	39,389 – 38,972	4 / 5	39,996 – 39,723	4 / 5
12.97-13.00	OxA-29322	39,622 – 39,216	4 / 5	40,123 – 39,861	4 / 5
13.00-13.05	OxA-29323	39,910 – 39,500	4 / 5	40,286 – 40,036	4 / 5
13.05-13.10	OxA-29324	40,362 – 39,842	11 / 5	40,482 – 40,248	16 / 5
13.10-13.15	OxA-29325	40,595 – 40,117	5 / 5	40,676 – 40,460	8 / 5
13.15-13.20	OxA-29326	40,781 – 40,364	5 / 5	40,870 – 40,672	7 / 5
13.20-13.25	OxA-29327	40,944 – 40,589	4 / 5	41,065 – 40,885	4 / 5
13.25-13.30	OxA-28847	41,127 – 40,589	8 / 5	41,262 – 41,095	10 / 5
	OxA-29603		3 / 5		3 / 5
13.30-13.35	OxA-29328	41,317 – 41,031	4 / 5	41,460 – 41,304	4 / 5
13.35-13.40	OxA-29329	41,530 – 41,241	5 / 5	41,660 – 41,512	4 / 5
13.40-13.45	OxA-29330	41,765 – 41,470	4 / 5	41,860 – 41,726	4 / 5
13.45-13.50	OxA-29331	41,996 – 41,677	5 / 5	42,061 – 41,939	5 / 5
13.50-13.55	OxA-29364	42,263 – 41,936	5 / 5	42,266 – 42,147	4 / 5
13.55-13.60	OxA-29365	42,551 – 42,240	4 / 5	42,469 – 42,355	4 / 5
13.60-13.65	OxA-29366	42,826 – 42,512	4 / 5	42,671 – 42,561	4 / 5
13.65-13.70	OxA-29367	43,101 – 42,770	5 / 5	42,875 – 42,765	4 / 5

Depth (m)	AMS Laboratory Code	Hulu Cave modelled age (cal. BP) using primary P_Sequence deposition model (68.2% range)	Posterior/prior Outlier probability (%)	Hulu Cave modelled age (cal. BP), using supporting U_Sequence deposition model (68.2% range)	Posterior/prior Outlier probability (%)
13.70-13.75	OxA-29368	43,385 – 43,037	5 / 5	43,080 – 42,969	4 / 5
13.75-13.80	OxA-28876	43,648 – 43,283	5 / 5	43,287 – 43,173	4 / 5
13.80-13.85	OxA-29369	43,896 – 43,519	5 / 5	43,496 – 43,375	4 / 5
13.85-13.90	OxA-29679	44,149 – 43,759	3 / 5	43,706 – 43,576	3 / 5
	OxA-29604		6 / 5		5 / 5
13.90-13.95	OxA-29370	44,435 – 44,025	4 / 5	43,915 – 43,777	4 / 5
13.95-14.00	OxA-29371	44,726 – 44,290	5 / 5	44,124 – 43,977	4 / 5
14.00-14.05	OxA-29372	45,021 – 44,560	5 / 5	44,335 – 44,178	4 / 5
14.05-14.10	OxA-29373	45,293 – 44,823	5 / 5	44,548 – 44,379	5 / 5
14.10-14.15	OxA-29374	45,535 – 45,071	5 / 5	44,762 – 44,580	5 / 5
14.15-14.20	OxA-30603	45,735 – 45,279	5 / 5	44,980 – 44,614	5 / 5
14.20-14.25	OxA-30604	45,930 – 45,465	5 / 5	45,197 – 44,805	5 / 5
14.25-14.30	OxA-30605	46,140 – 45,643	5 / 5	45,412 – 44,997	5 / 5
14.30-14.35	OxA-30606	46,372 – 45,832	5 / 5	45,626 – 45,190	5 / 5
14.35-14.40	OxA-30607	46,606 – 46,010	6 / 5	45,840 – 45,382	6 / 5
14.40-14.45	OxA-30761	46,867 – 46,220	5 / 5	46,052 – 45,579	5 / 5
14.45-14.50	OxA-30762	47,141 – 46,451	5 / 5	46,265 – 45,769	5 / 5
14.50-14.55	OxA-30763	47,410 – 46,684	5 / 5	46,479 – 45,961	5 / 5
14.55-14.60	OxA-30764	47,692 – 46,942	5 / 5	46,692 – 46,156	4 / 5
14.60-14.65	OxA-30765	47,970 – 47,192	5 / 5	46,905 – 46,350	5 / 5
14.65-14.70	OxA-29698	48,272 – 47,446	5 / 5	47,119 – 46,541	4 / 5
14.70-14.75	OxA-30766	48,563 – 47,681	5 / 5	47,333 – 46,735	5 / 5
14.75-14.80	OxA-29699	48,858 – 47,915	5 / 5	47,547 – 47,025	5 / 5

Table S4. IntCal13 (Reimer et al., 2013) modelled ages for our contiguous, homogenised peat samples from Tenaghi Philippon core TP-2005, as derived from the `P_Sequence` (model B) and supporting `U_Sequence` (model F) deposition models in OxCal ver. 4.3 (Bronk Ramsey, 2008, 2019; Bronk Ramsey and Lee, 2013). (N.b. the supporting measurements of the base-soluble humic acid component extracted from the peat, as given in Table S2, were not included in the Bayesian modelling.) For simplicity, the modelled data are presented at the 68.2% highest probability density ranges. Posterior `Outlier` probabilities for each ^{14}C determination are given, as compared to the prior 5% probabilities applied to each sample.

Depth (m)	AMS Laboratory Code	IntCal13 modelled age (cal. BP) using primary `P_Sequence` deposition model (68.2% range)	Posterior/prior `Outlier` probability (%)	IntCal13 modelled age (cal. BP), using supporting `U_Sequence` deposition model (68.2% range)	Posterior/prior `Outlier` probability (%)
12.87-12.90	OxA-28873	38,578 – 38,990	4 / 5	38,751 – 39,089	4 / 5
12.90-12.92	OxA-29318	38,675 – 39,069	4 / 5	38,872 – 39,200	4 / 5
12.92-12.94	OxA-29319	38,740 – 39,137	3 / 5	38,958 – 39,278	4 / 5
	OxA-29320		9 / 5		13 / 5
12.94-12.97	OxA-29321	38,910 – 39,344	4 / 5	39,096 – 39,406	4 / 5
12.97-13.00	OxA-29322	39,170 – 39,636	4 / 5	39,265 – 39,565	4 / 5
13.00-13.05	OxA-29323	39,514 – 39,997	5 / 5	39,485 – 39,768	4 / 5
13.05-13.10	OxA-29324	40,041 – 40,499	8 / 5	39,748 – 40,014	21 / 5
13.10-13.15	OxA-29325	40,295 – 40,704	5 / 5	40,011 – 40,260	6 / 5
13.15-13.20	OxA-29326	40,500 – 40,880	5 / 5	40,275 – 40,506	6 / 5
13.20-13.25	OxA-29327	40,670 – 41,030	5 / 5	40,535 – 40,755	4 / 5
13.25-13.30	OxA-28847	40,854 – 41,191	8 / 5	40,797 – 41,002	9 / 5
	OxA-29603		3 / 5		2 / 5
13.30-13.35	OxA-29328	41,020 – 41,350	5 / 5	41,057 – 41,251	4 / 5
13.35-13.40	OxA-29329	41,196 – 41,527	5 / 5	41,316 – 41,502	4 / 5
13.40-13.45	OxA-29330	41,410 – 41,745	5 / 5	41,574 – 41,754	4 / 5
13.45-13.50	OxA-29331	41,596 – 41,941	5 / 5	41,830 – 42,005	5 / 5
13.50-13.55	OxA-29364	41,850 – 42,217	5 / 5	42,083 – 42,261	4 / 5
13.55-13.60	OxA-29365	42,185 – 42,560	5 / 5	42,335 – 42,517	4 / 5
13.60-13.65	OxA-29366	42,479 – 42,860	5 / 5	42,585 – 42,774	4 / 5
13.65-13.70	OxA-29367	42,744 – 43,146	5 / 5	42,835 – 43,033	4 / 5

Depth (m)	AMS Laboratory Code	IntCal13 modelled age (cal. BP) using primary P_Sequence deposition model (68.2% range)	Posterior/prior Outlier probability (%)	IntCal13 modelled age (cal. BP), using supporting U_Sequence deposition model (68.2% range)	Posterior/prior Outlier probability (%)
13.70-13.75	OxA-29368	43,034 – 43,449	5 / 5	43,084 – 43,292	4 / 5
13.75-13.80	OxA-28876	43,279 – 43,715	5 / 5	43,330 – 43,554	5 / 5
13.80-13.85	OxA-29369	43,495 – 43,949	5 / 5	43,577 – 43,815	4 / 5
13.85-13.90	OxA-29679	43,725 – 44,195	3 / 5	43,824 – 44,076	3 / 5
	OxA-29604		6 / 5		5 / 5
13.90-13.95	OxA-29370	44,007 – 44,496	5 / 5	44,069 – 44,340	4 / 5
13.95-14.00	OxA-29371	44,298 – 44,805	5 / 5	44,315 – 44,603	4 / 5
14.00-14.05	OxA-29372	44,609 – 45,118	5 / 5	44,560 – 44,866	4 / 5
14.05-14.10	OxA-29373	44,883 – 45,382	5 / 5	44,805 – 45,130	5 / 5
14.10-14.15	OxA-29374	45,110 – 45,596	5 / 5	45,050 – 45,395	6 / 5
14.15-14.20	OxA-30603	45,283 – 45,773	5 / 5	45,295 – 45,661	5 / 5
14.20-14.25	OxA-30604	45,420 – 45,922	5 / 5	45,540 – 45,926	5 / 5
14.25-14.30	OxA-30605	45,561 – 46,087	5 / 5	45,783 – 46,190	5 / 5
14.30-14.35	OxA-30606	45,720 – 46,276	5 / 5	46,026 – 46,456	4 / 5
14.35-14.40	OxA-30607	45,875 – 46,473	6 / 5	46,270 – 46,720	7 / 5
14.40-14.45	OxA-30761	46,064 – 46,709	5 / 5	46,515 – 46,985	5 / 5
14.45-14.50	OxA-30762	46,270 – 46,964	5 / 5	46,758 – 47,251	5 / 5
14.50-14.55	OxA-30763	46,491 – 47,234	5 / 5	47,002 – 47,517	5 / 5
14.55-14.60	OxA-30764	46,727 – 47,523	5 / 5	47,246 – 47,783	4 / 5
14.60-14.65	OxA-30765	46,958 – 47,813	5 / 5	47,490 – 48,047	5 / 5
14.65-14.70	OxA-29698	47,191 – 48,114	5 / 5	47,732 – 48,314	4 / 5
14.70-14.75	OxA-30766	47,413 – 48,414	5 / 5	47,977 – 48,580	4 / 5
14.75-14.80	OxA-29699	47,622 – 48,709	5 / 5	48,221 – 48,847	4 / 5

Fig. S1. Reconstructed atmospheric ^{14}C concentrations ($\Delta^{14}C$) based on Tenaghi Philippon core TP-2005 as modelled against the Hulu Cave dataset of Cheng et al. (2018; pink curve) using: i) the primary poisson process (`P_Sequence`) deposition model (green data points; model A); and ii) the supporting uniform (`U_Sequence`) deposition model (blue data points; model E). For clarity, all data are plotted at 68.2%/1σ probability ranges. See section 3.2 of the main text for further discussion.

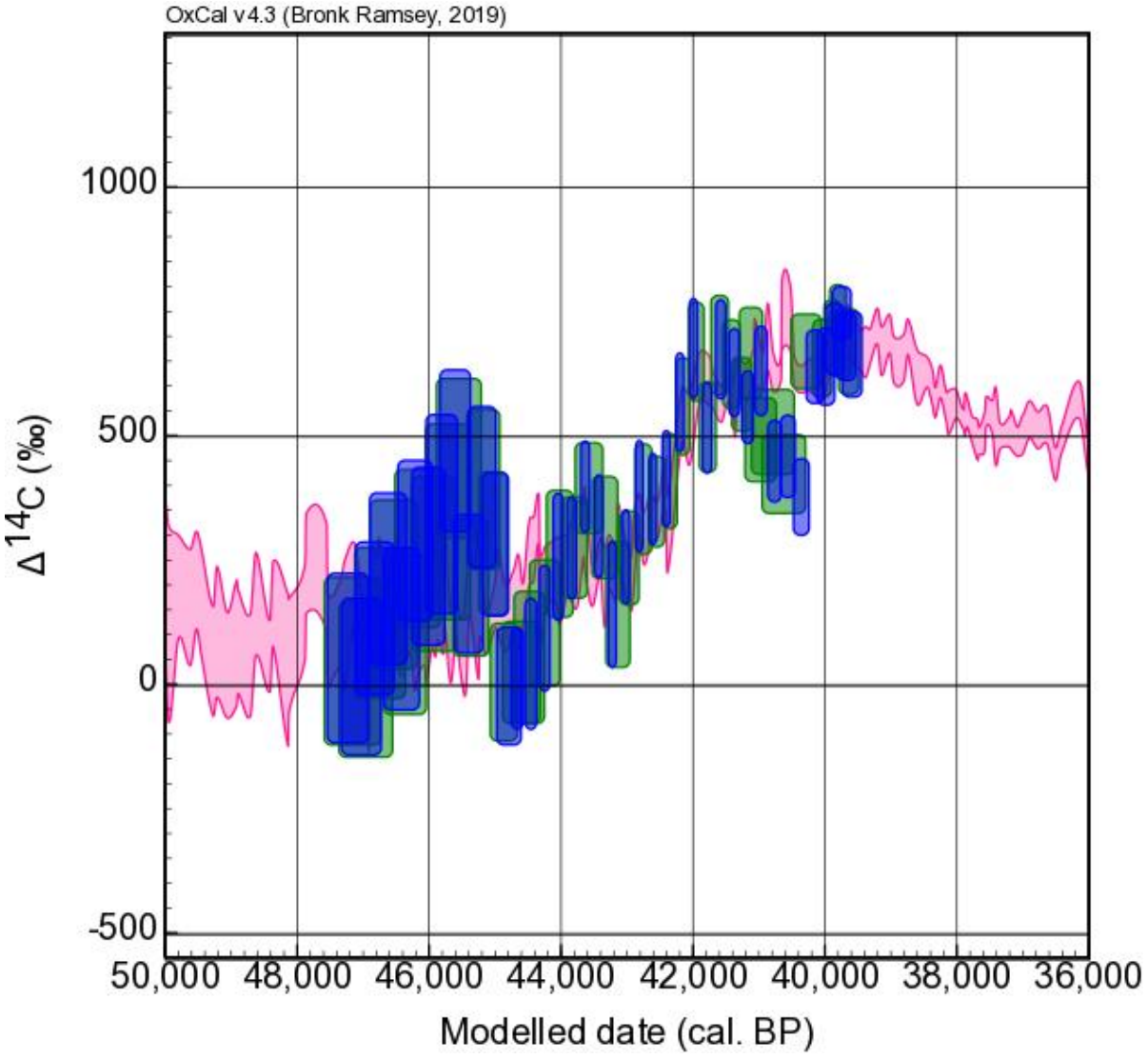

Fig. S2. Reconstructed atmospheric ^{14}C concentrations ($\Delta^{14}C$) based on Tenaghi Philippon core TP-2005 as modelled against IntCal13 (Reimer et al., 2013; red curve) using: i) the primary poisson process (`P_Sequence`) deposition model (green data points; model B); and ii) the supporting uniform (`U_Sequence`) deposition model (blue data points; model F). For clarity, all data are plotted at 68.2%/1σ probability ranges. See section 3.2 of the main text for further discussion.

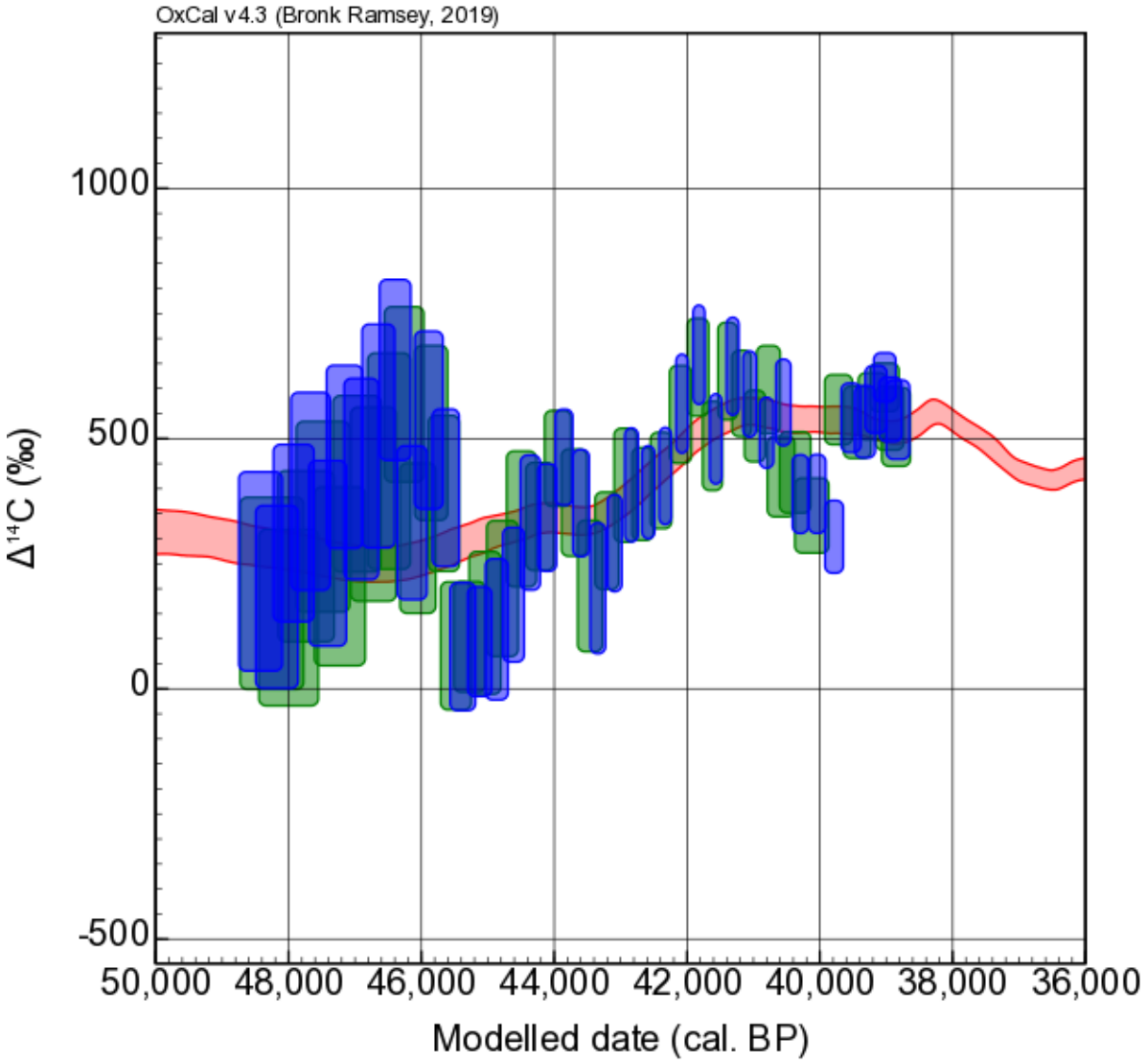

Fig. S3. Revised age-depth profile (green) for core TP-2005 from Tenaghi Philippon, as compared to the previously published dataset of Müller et al. (2011; red), generated by independent P_Sequence deposition modelling in OxCal ver. 4.3 (Bronk Ramsey, 2008, 2019; Bronk Ramsey and Lee, 2013) on to: **(a)** the Hulu Cave ^{14}C calibration dataset of Cheng et al. (2018); and **(b)** the IntCal13 calibration curve (Reimer et al., 2013). Modelled data are plotted in bold, overlying the unmodelled probability density functions with the 68.2% highest probability density range interpolations overlain.

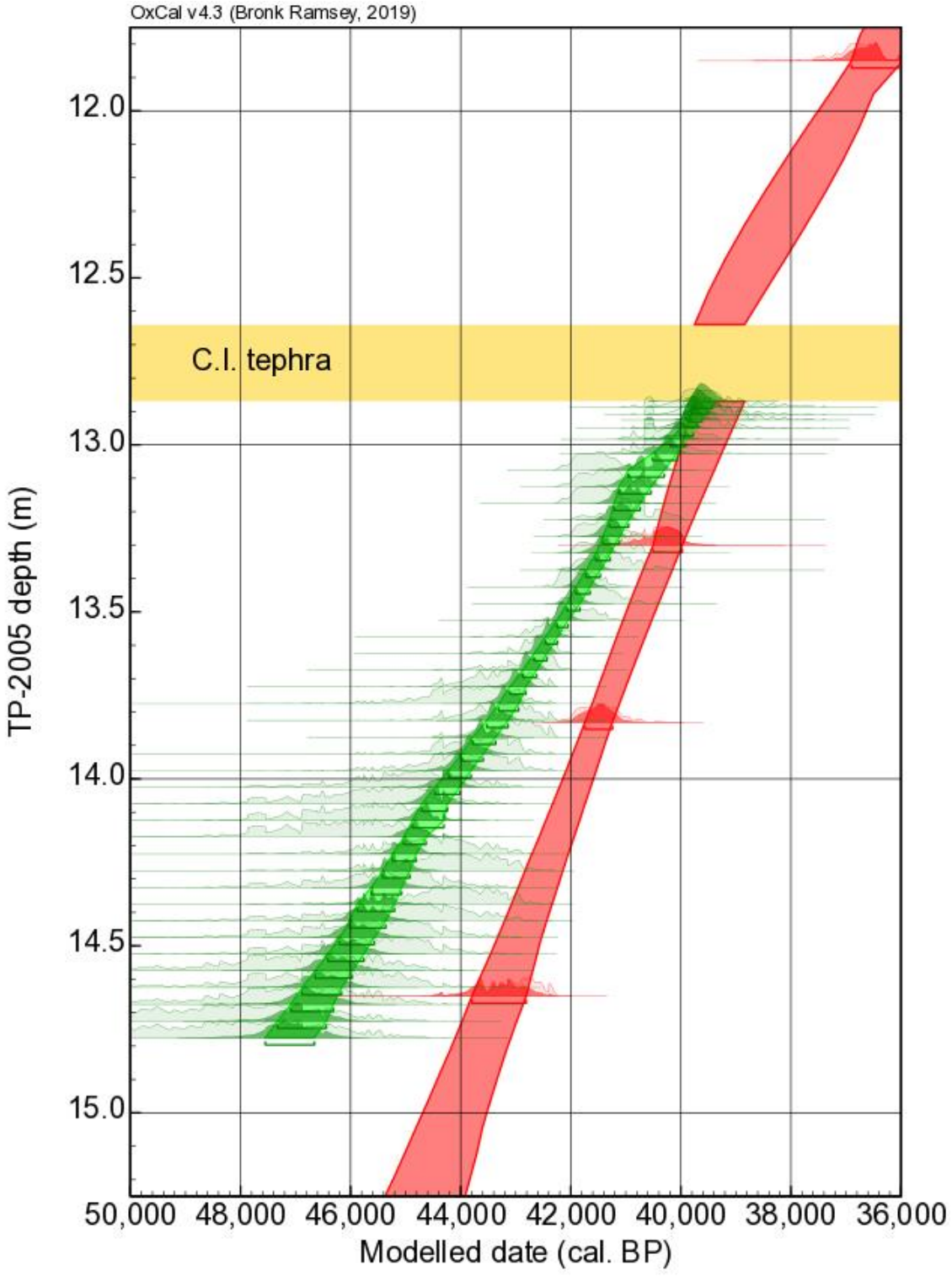

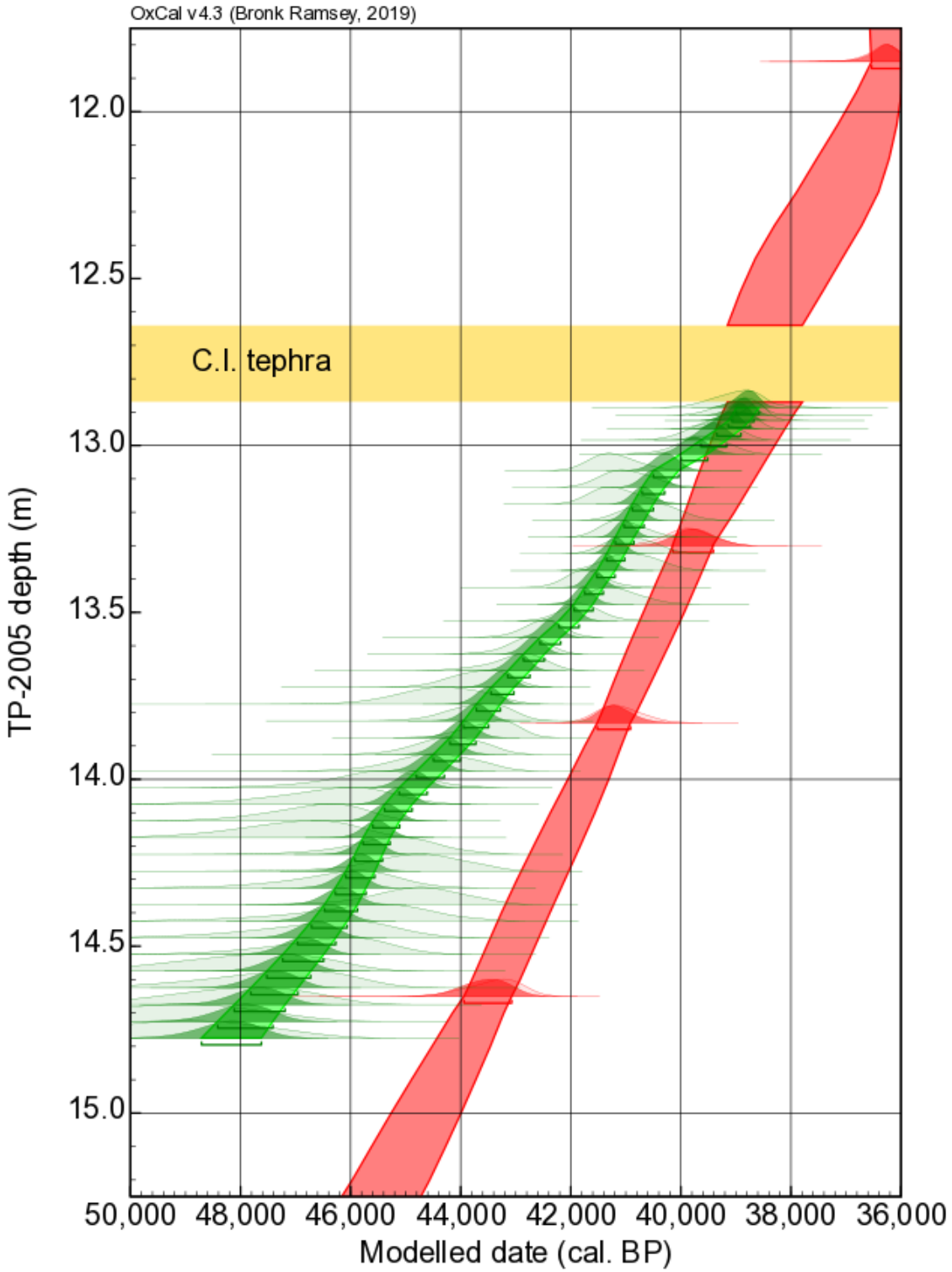
OxCal v4.3 (Bronk Ramsey, 2019)
C.I. tephra
TP-2005 depth (m)
12.0
12.5
13.0
13.5
14.0
14.5
15.0
50,000
48,000
46,000
44,000
42,000
40,000
38,000
36,000
Modelled date (cal. BP)

27
28

Fig. S4. The contributory ^{14}C datasets to IntCal13 (Reimer et al., 2013) (grey curve) between 50,000 and 36,000 cal. BP: Lake Suigetsu (Bronk Ramsey et al., 2012) (green triangles); Bahamas speleothem (Hoffmann et al., 2010) (gold squares); Cariaco Basin foraminifera (Hughen et al., 2006) (cyan circles); and marine corals (Fairbanks et al., 2005) (blue squares). (For clarity, all data are plotted at 68.2%/1σ probability ranges.)

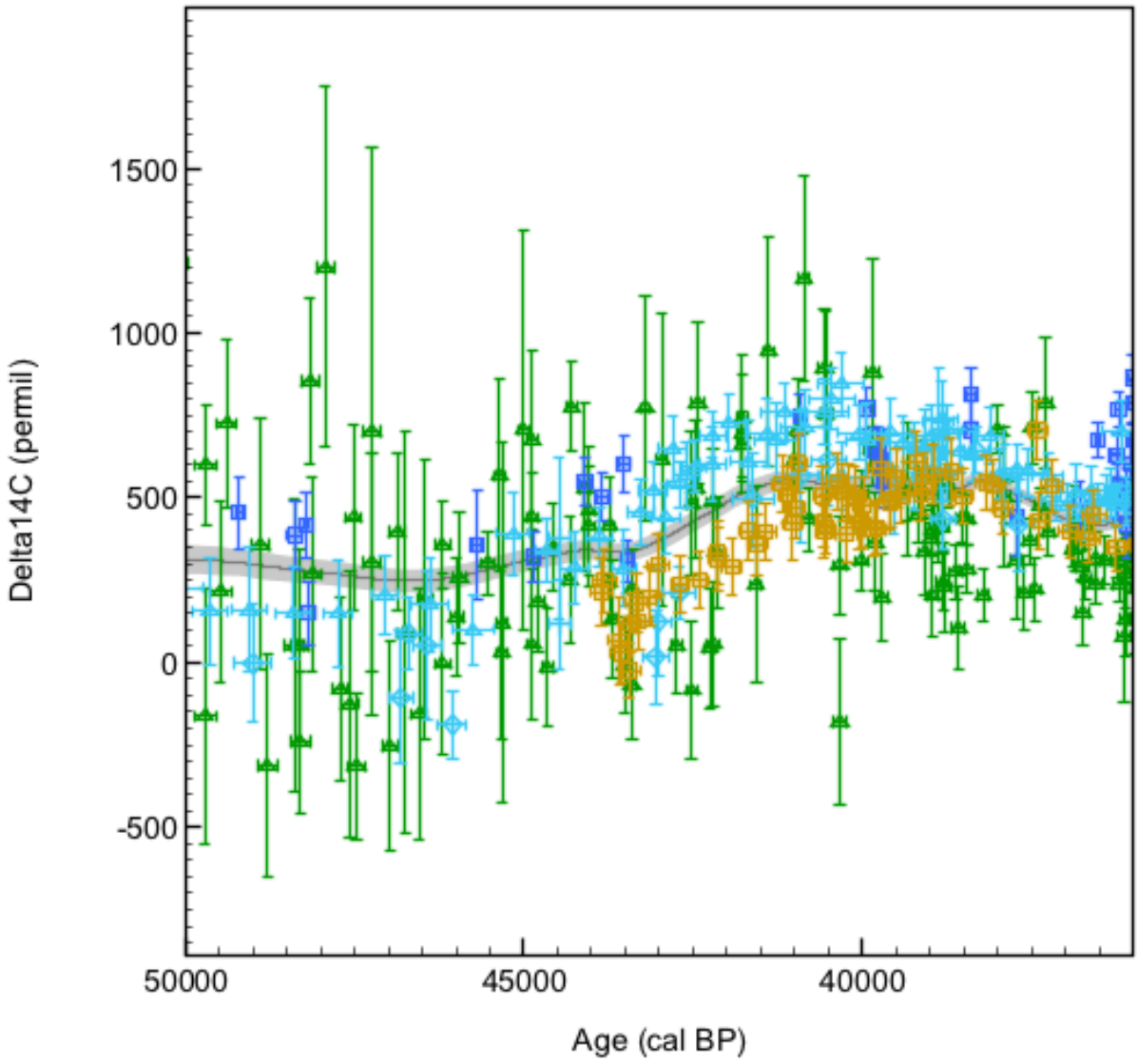

Fig. S5. Estimation of the age of the Campanian Ignimbrite (C.I.) tephra based on: **(a)** our new ^{14}C data from Tenaghi Philippon (core TP-2005) as modelled on to the Hulu Cave dataset of Cheng et al. (2018); and **(b)** as modelled on to IntCal13 (Reimer et al. 2013); as compared to: **(c)** the original, low resolution TP-2005 ^{14}C data of Müller et al. (2011) modelled on to IntCal13; **(d)** the Black Sea record of Black Sea record of Nowaczyk et al. (2012, 2013) on the GICC05 timescale; **(e)** the $^{40}Ar/^{39}Ar$ age of 39,790 ± 140 years BP produced by Giaccio et al. (2017); and **(f)** the widely quoted $^{40}Ar/^{39}Ar$ age of De Vivo et al. (2001). (Horizontal bars beneath each distribution represent the 68.2%, 95.4% and 99.7% highest probability density ranges, respectively, and the crosses plot the median ages.)

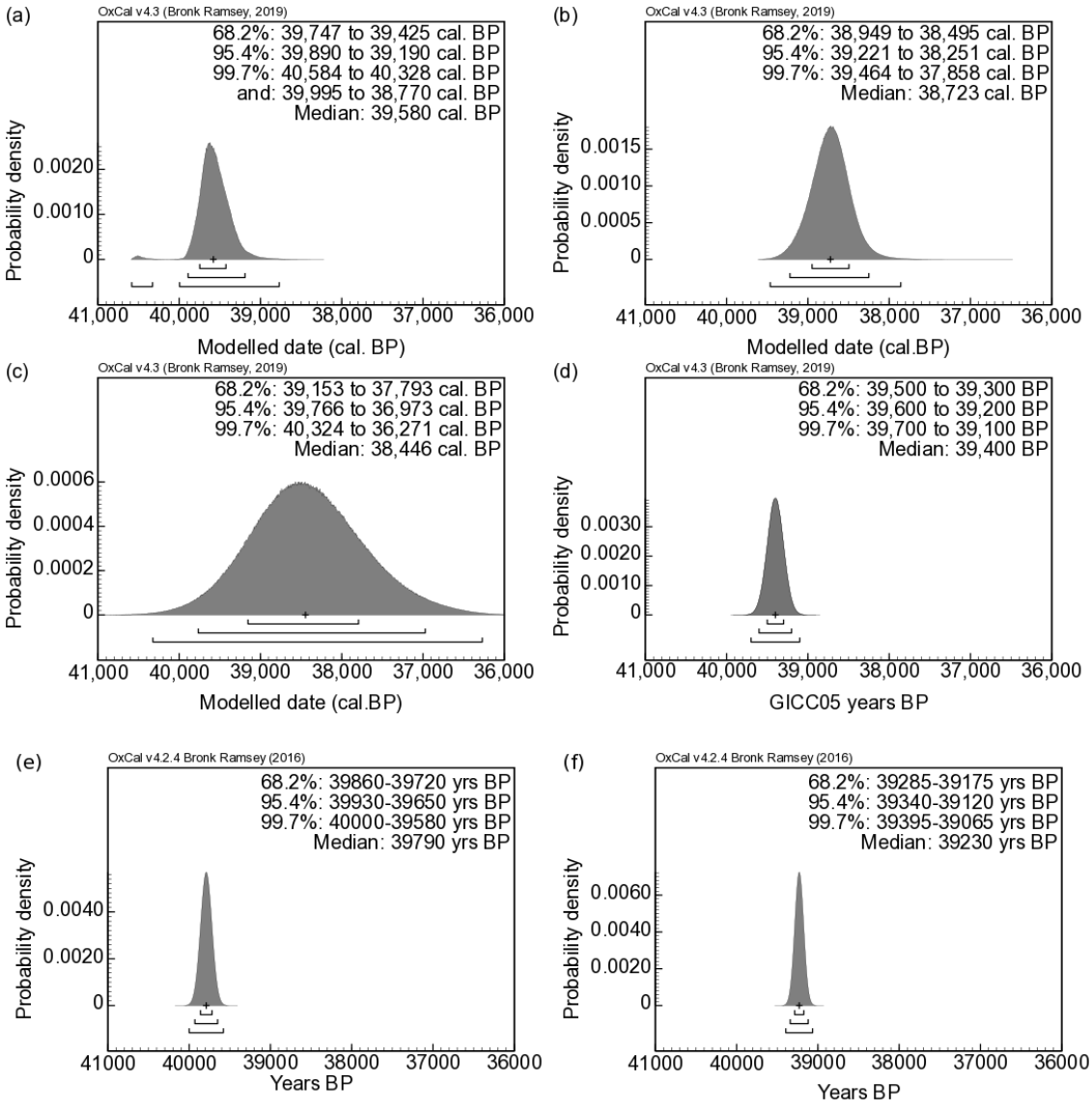

Fig. S6. The difference between our Tenaghi Philippon (core TP-2005) ^{14}C-inferred age for the Campanian Ignimbrite (C.I.) tephra:
(i) on the Hulu Cave U-series timescale of Cheng et al. (2018) and: **(a)** the widely quoted ^{40}Ar/^{39}Ar age of De Vivo et al. (2001; 39,230 ± 110 years BP, before AD 1950, 2σ); and **(b)** the recent ^{40}Ar/^{39}Ar age of Giaccio et al. (2017; 39,790 ± 140 years BP, before AD 1950, 95.4% range);
and (ii) on the IntCal13 timescale (Reimer et al. 2013), compared with the same ^{40}Ar/^{39}Ar ages, **(c)** that of De Vivo et al. (2001); and **(d)** that of Giaccio et al. (2017).
(Horizontal bars beneath each probability distribution represent the 68.2%, 95.4% and 99.7% highest probability density ranges, respectively, and the cross plots the median age difference.)

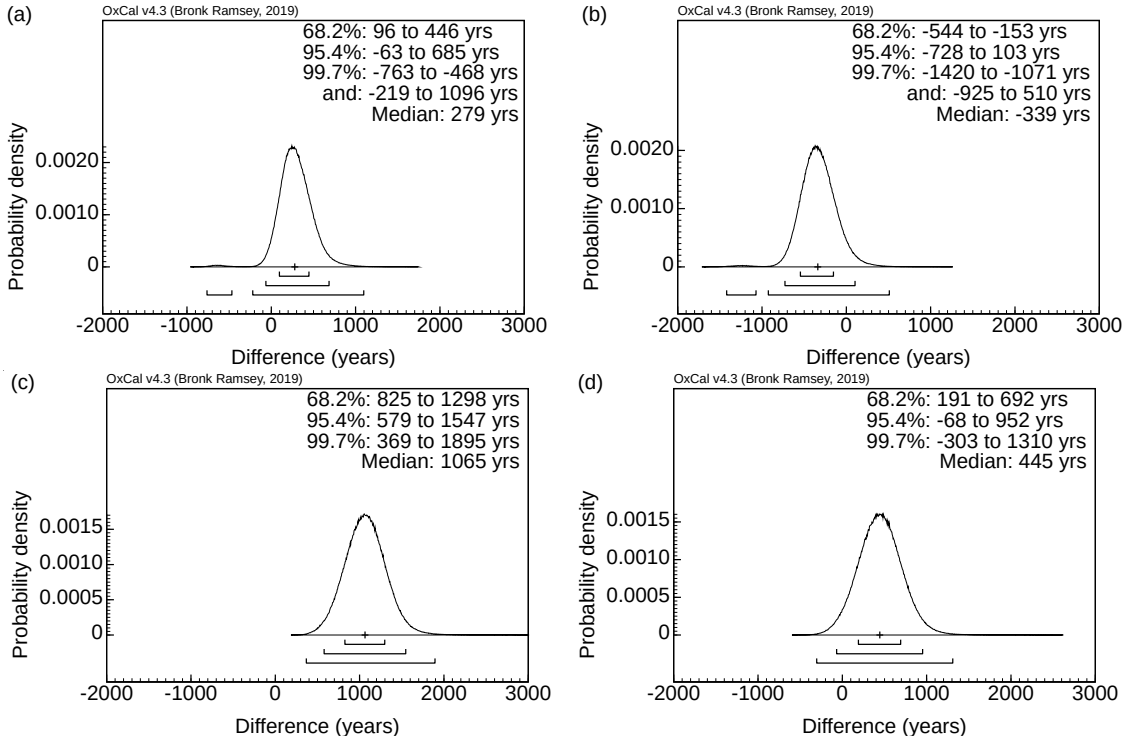

SUPPLEMENTARY REFERENCES (further to those listed in main text)

Reimer PJ, Brown TA, Reimer RW (2004) Discussion: reporting and calibration of post-bomb ^{14}C data. Radiocarbon 46(3):1299-1304, https://journals.uair.arizona.edu/index.php/radiocarbon/article/view/4183/3608.

Stuiver M, Polach HA (1977) Reporting of ^{14}C Data. Radiocarbon 19(3):355-263, https://journals.uair.arizona.edu/index.php/radiocarbon/article/view/493/498.